NUCLEAR MAGNETIC RESONANCE IMAGING: APPLICATION TO DETERMINATION OF SATURATION CHANGES IN A SANDSTONE CORE BY SEQUENTIAL WATERFLOODING

Nina Loahardjo and Norman R. Morrow, University of Wyoming
James Stevens and James Howard, ConocoPhillips

This paper was prepared for presentation at the International Symposium of the Society of Core Analysts held in Halifax, Nova Scotia, Canada, 4-7 October, 2010

ABSTRACT

Sequential waterfloods are performed by waterflooding followed by re-establishment of high oil saturation, followed by further waterflooding and so on; the core is not restored by core cleaning and re-aging between consecutive floods. Even when there is no change in salinity, laboratory tests for both sandstone and limestone usually showed increase in oil recovery from one flood to the next. Oil recovery was determined volumetrically.

As an independent check on the material balance, sequential waterflooding was tested on Berea Sandstone at elevated temperature using Nuclear Magnetic Resonance Imaging (MRI) to determine *in situ* changes in initial and final saturation profiles for each flood. The MRI signal from water was blocked by using brine prepared with heavy water (D_2O). Four cycles of waterflooding were performed at elevated temperature. The residual oil saturations, determined from imaging the whole sample (referred to as 3D imaging), were 36.2% after the first waterflood and 28.8% and 24.0% respectively for the second and third cycle. A 4^{th} flood was run in which a limited volume of oil was injected at the outlet end of the core followed by water injection in the same direction; the residual oil saturation was 21.9%. The residual oil saturation after the fourth cycle was subsequently checked by a tracer test technique; the value obtained, 23.0%, was in close agreement with the value of 21.9% obtained by 3D imaging.

The initial oil distribution, the distribution at breakthrough, and at residual oil saturation, show that for each consecutive waterflood, an increasing fraction of oil recovery occurs after breakthrough. This and other observations related to the mechanism of increased oil recovery by sequential waterflooding are discussed.

INTRODUCTION

Waterflooding is by far the most widely applied method of improving oil recovery. Significant quantities of oil, typically, more than one-half of the original oil in place, remain in the reservoir after waterflooding and are commonly the target for improved oil recovery processes.

Loahardjo [1] and Loahardjo et al. [2] reported increases in recovery of crude oil for sequential floods of sandstones and limestone (Figure 1) for which there was no change in salinity and no re-aging between each flood. The results were based on volumetric material balance. Demonstration of increased oil recovery by an independent measure of saturation change would provide increased confidence in the volumetric data.

In situ changes in saturation during a laboratory flood experiment were determined by Nuclear Magnetic Resonance Imaging (MRI). This technique provided measurement of end point saturations and visualization of the advance of the fluid front during waterflooding and the resulting saturation distribution along the core.

EXPERIMENTAL

Crude Oil

The properties of the crude oil, designated as WP, are summarized in Table 1. The crude oil was filtered to remove particulate matter and then held under vacuum for 2 hours at room temperature to minimize the possibility of gas evolution during the course of displacement at a displacement temperature of 60°C. At this temperature, the vapor pressure of the degassed oil is 2.2 psi and the viscosity is 28.2 cP.

Table 1. Crude Oil Properties

Crude Oil	WP
C_6 asphaltenes, % weight	6.3
Acid #, mg KOH/ g oil	1.46
Base #, mg KOH/ g oil	2.49
ρ at 22°C, g/cm^3	0.9125
μ oil at 22°C, cP	112.2
μ oil at 60°C, cP	28.2

Brine

The core for the MRI experiments was saturated using synthetic seawater of 35,493 ppm Total Dissolved Solids (TDS) prepared with deuterium oxide, D_2O, in order to eliminate the MRI signal from the brine. The aqueous phase can then be distinguished from the oil phase, because the only detectable MRI signal is from the oil. Sodium azide, NaN_3, was added as a biocide to prevent bacterial growth (Table 2). The brine was degassed by vacuum. The same brine was used as the connate and injection brine and there was no change in brine composition throughout the test. The viscosity of the brine was about 0.6 cP at 60°C. The crude oil/brine interfacial tension was 28.18 mN/m.

Core

A core of 1.5 inches diameter and about 3.0 inches in length was cut from a block of Berea sandstone using tap water as the cutting fluid. After cutting, the core was dried at 110°C for 1-2 days, and allowed to cool in a vacuum desiccator. Permeability to nitrogen

was 518 mD. The core was saturated under vacuum with brine and left to soak in the brine for at least 14 days to allow equilibration between the rock minerals and the brine. The porosity, calculated from the weight difference between the dry and saturated core, was 21%. Thin section analysis indicated that the sandstone contains quartz, mica, feldspar, carbonate cementation, rock fragments and is also rich in kaolinite.

Table 2. . D_2O-Brine Composition

Composition [g/L]	**Seawater**
NaCl	28
KCl	0.935
$CaCl_2$	1.19
$MgCl_2$	5.368
NaN_3	0.1
TDS /L	35.493

Establishing Initial Water Saturation

Initial water saturation, S_{wi}, was first established at room temperature by flooding with 4 pore volumes (PV) of WP crude oil at 2 cm^3/min. The core was then flooded with 1 PV in the reverse direction to mitigate possible end effects and also to minimize any saturation gradient along the core. The oil permeability, k_o, measured during establishment of S_{wi} was 241 mD. The initial water saturation prior to the first cycle was determined by volumetric balance and also checked gravimetrically. Initial water saturation was established at 60^{o}C for subsequent test cycles.

Aging

After establishing S_{wi} the core was removed from the core holder and submerged in crude oil in a sealed pressure vessel. The pressure was then raised to 900 psi to ensure that any gas left in the core passed into solution. The core was then aged (T_a = 75^{o}C) for 14 days.

Waterfloods

After aging, the core was set in the core holder at 60^{o}C with 300 psi confining pressure and then waterflooded at 0.25 cm^3/min. During the waterflood, the pressure drop across the core was recorded. The displacement temperature, T_d, was 60^{o}C. An individual cycle, C, of sequential flooding was defined as flooding with brine followed by re-establishment of an initial water saturation by flow of crude oil. In the present work the core was not restored by cleaning and re-aging between cycles; the single restoration step, performed at the outset, is indicted as R1.

Nuclear Magnetic Resonance Imaging

The Nuclear Magnetic Resonance Imaging (MRI) test was run at ConocoPhillips Technology Center in Bartlesville, Oklahoma, USA. The MRI instrument is a Unity/Inova Imaging 85/310 spectrometer, Varian Inc., Palo Alto, CA (modified, after

Ersland, 2008 [3]). MRI images were obtained for two dimensional slices of about 1 cm width in the x-y-plane along the middle of the core. Two-dimensional (2D) profile images were acquired to examine the frontal flow behavior and the distribution of oil and water along the core during the water and oil floods. During waterflooding, data for the 2D slice were usually acquired every 8 minutes. During re-establishment of initial water saturation by oilflooding, the 2D profile was generally acquired every 4 minutes. Three dimensional (3D) imaging was also used at the stable end-point saturations to give high quality saturation profiles and to obtain initial brine and residual oil saturations for the whole core volume. Each of these 3D static profiles was acquired within 1 hour. Average signals obtained after correction for noise, were used to improve the resolution of the images.

The initial water saturation, S_{wi}, and the residual oil saturation, S_{or}, extracted from the 2D and 3D images were normalized against known saturation values. The key factor in the interpretation is that image intensity over the bulk sample is linearly correlated with saturation.

RESULTS

MRI has been applied to determine *in situ* changes in saturation and also to visualize the fluid distribution and frontal behavior for a laboratory waterflood. A test of sequential waterflooding was performed on a Berea sandstone core designated as BS 10. A series of images displaying waterflood and oilflood processes provided images of the fluid frontal behavior and recovery after breakthrough. Decreasing signal intensity was evidence of displacement of oil by brine during waterflooding. Increasing signal intensity during oilflooding showed the progress of establishment of the initial brine saturation.

R1/C1

Core BS 10 was saturated with D_2O-brine and allowed to equilibrate for 14 days. An initial water saturation (S_{wi} = 26.0%) was established by flow of WP crude oil, which had a viscosity of 112.2 cP at room temperature. The core was aged for 21 days at 75^{o}C in a pressure vessel and was then set in the core holder inside the MRI unit. The temperature was raised to 60^{o}C. 1D, 2D, and 3D images for initial and residual saturations are shown in Figure 2. The fluid distributions were uniform. The initial water saturation determined by 2D and 3D imaging for this cycle were used as reference values for subsequent evaluation of changes in saturation.

1D and 2D profiles, imaged at 8 minute intervals during the D_2O-brine displacement, are shown in Figures 3 and 4 respectively. The flow direction was from right to left. The D_2O-brine was injected at 0.25 cm^3/min. After 0.12 PV injection of brine, the brine front had advanced along about one quarter of the length of the core. Water breakthrough occurred after injection of 0.48 PV of brine. Up to the time of water breakthrough, the saturation front remained sharp. Figure 2 shows 1D/2D and 3D profiles at residual oil saturation. The residual oil saturation was 36.9% from the 2D profile and 36.2% from the 3D profile.

R1/C2

Initial water saturation for the second cycle was re-established by oil flooding at 2 cm^3/min at 60°C. For the first 8.53 PV injection, the flow was from right to left (see Figure 5); then, the flow direction was reversed to mitigate end effects. Even though the image was taken every 4 minutes, the oil front was not identified in detail because of the high oil flow rate used to establish the initial brine saturation. The saturation profiles showed very little change with reversal of the direction of oil flooding. This implied that any retention of brine because of end effects was small. From the 2D profile shown in Figure 2, the initial water saturation (S_{wi}) was 29.7%. The 3D profiles shown in Figure 2 gave slightly smaller initial water saturation (S_{wi} = 27.2%).

For water injection, instead of the sharp water front given by the water injection step for Cycle C1, the advancing water front for R1/C2 was more disperse (Figures 3 and 4). The oil recovery for R1/C2 was higher than for R1/C1. The residual oil saturation was 25.1% from 2D profiles and 28.8% from the 3D profile for R1/C2 (Figure 2).

R1/C3

An initial water saturation was established using the same flow conditions as for Test R1/C2. The initial water saturation was 29.5% from the 2D image and 27.6% from the 3D image (Figure 2). The oil front was still visible in the second image for R1/C3, obtained after 8 minutes.

The fluid distribution which developed during the course of waterflooding is shown in Figures 3 and 4. At the end of the waterflood, from 2D profiles, the residual oil saturation had decreased from 25.1% for R1/C2 to 20.0% for R1/C3; from the 3D profiles the residual oil saturation decreased from 28.8% for R1/C2 to 24.0% for R1/C3 (Figure 2).

R1/C4

0.71 PV of crude oil was directly injected for 6 minutes into the outlet side of the core (from left to right) at 60°C to re-establish the initial water saturation for Test R1/C4 (Figure 5). The direction of crude oil flow was not reversed. During this time, the images were taken at 1 minute intervals. A sharp oil front was observed. Within 6 minutes, the crude oil saturation had risen along the whole core length (Figure 5). Figure 2 gave 40.2% and 35.1% initial water saturation from the 2D and the 3D profiles respectively, indicating, as expected, that the injection of less than a PV of oil resulted in a relatively high and heterogeneous distribution of the initial water compared to the previous three flooding cycles.

As for the oil flood, the waterflood was also run in the reverse direction to the previous three waterfloods (cf. Figures 3 and 4). For Test R1/C4, the invading brine front was distinctly more disperse than for the previous three waterfloods (cf. Figures 3 and 4). The residual oil saturation for R1/C4 was 16.0% and 21.9% from the 2D and 3D images respectively (Figure 2).

In addition to the MRI values, the residual oil saturation after the fourth cycle was determined by a tracer test [4,5]. The separation of co-injected methyl alcohol and ester are shown in Figure 6. The value obtained by history matching the production profile gave a residual oil of 23.0%, which was very close to the value of 21.9% obtained after the fourth cycle by 3D imaging.

DISCUSSION

Saturation changes were tracked by recording 1D and 2D profiles every 4 or 8 minutes. This procedure gave images with satisfactory resolution. However, these intervals set limitation on capturing the exact time of breakthrough as indicated by the presence of the invading liquid along the whole length of the core. (Better time-resolution of a flood could be obtained by using faster MRI acquisition times, slower injection rates, or a longer core.)

The final initial brine and residual oil saturations determined for each cycle from the MRI images are listed in Table 3. Initial and final saturation versus cycle number are plotted in Figure 7. The trends obtained either from 2D images taken during the course of flooding or 3D images given by beginning or end point saturations, are in agreement for both initial water saturation and residual oil saturation. The initial water saturation values from MRI for both 2D and 3D images by flooding with oil at 60°C (μ_{oil} = 28.2 cP) show less overall variation than when established by flooding with oil at ambient temperature (μ_{oil} = 112.2 cP) [6]. The 3D values of residual oil, based on whole core imaging, were adopted for comparison with core flood results based on material balance.

Even though the initial water saturations, S_{wi}, for the first three cycles were almost the same, the crude oil and brine flow behavior as revealed by the saturation profiles show changes. For Test R1/C1, up to the time of water breakthrough, the saturation fronts were sharp so the displacement process was essentially piston like.

Table 3. S_{wi} and S_{or} from 2D and 3D profiles

Cycle	S_{wi}		S_{or}	
	2D	3D	2D	3D
R1/C1	0.26	0.26	0.37	0.36
R1/C2	0.30	0.27	0.25	0.29
R1/C3	0.30	0.28	0.20	0.24
R1/C4	0.40	0.35	0.16	0.22

For the second and subsequent cycles, the water front before breakthrough became more diffuse from one cycle to the next. The 1D profile at breakthrough from Figure 8 was compared with the 1D profile obtained at residual oil saturation for each cycle. For Test R1/C1, there was clean water breakthrough and no further change in the 1D profile after breakthrough. However, for Tests R1/C2 and R1/C3, oil continued to be produced after breakthrough with reduction in oil saturation along the whole length of the core.

The overall changes in the profiles and oil recoveries imply that there was change in the displacement mechanism for consecutive waterfloods.

For Test R1/C4 (0.71 PV oil injection), the initial water saturation was 35% from the 3D image and 40% from the 2D image. These higher values, relative to those for previous cycles, were expected because of the small volume of injected oil. The fluid distribution at the outset of the waterflood was more heterogeneous than for the previous tests, but the final oil distribution was uniform.

Each consecutive cycle for the sandstone resulted in systematic increase in recovery of crude oil with corresponding decrease in residual oil. The oil recovery curves given by 2D images for each cycle are shown in Figure 9. The phenomena of reduction in residual oil saturation observed for sequential core floods using volumetric material balance were confirmed by both the 2D and 3D images. The values of residual oil saturations from the 3D images for each cycle are plotted together with previous sequential waterflooding results given by Edwards limestone, and Berea and Bentheim sandstone (Figure 10) [1]. Reductions in residual oil saturation were observed for displacement temperatures of 60^{o}C. All of the tests were run with core that had been aged at elevated temperature (75^{o}C) for at least 14 days.

Aging a core at residual oil saturation causes increase in rate of and extent of spontaneous imbibition (Figure 11) [6] indicating that the core became more water-wet with aging at high water saturation. Changes in flow behavior for the second cycle of flooding shown by the 1D profile (Figure 8) indicate change in wettability for consecutive cycles of flooding. It appears that increased recovery results from a form of change in wettability towards increased water wetness that is favorable to recovery.

The more conservative 3D image values are still encouraging with respect to practical application of sequential waterflooding. From Table 3, the initial oil saturation at the start of R1/C1 was 0.74. Based on the 3D images, the residual oil saturation after Test R1/C1 was 36% and the residual oil saturation after test R1/C2 was 29%. Therefore, the % incremental increased in recovery, % ΔS_{oe} [7], is:

$$\%\Delta S_{oe} = \frac{\left(S_{orR1/C1} - S_{orR1/C2}\right)}{\left(S_{oi} - S_{orR1/C2}\right)} 100\% = \frac{\left(0.36 - 0.29\right)}{\left(0.74 - 0.36\right)} 100\% = 18.4\%$$

Further imaging studies will be made to obtain saturation profiles for other conditions of sequential flooding that have been found to give increased oil recovery. The mechanism of increased oil recovery is also being investigated through detailed examination of pore structure and displacement at the pore and sub-pore scale by micro X-ray CT imaging techniques [8,9].

CONCLUSIONS

1. Nuclear Magnetic Resonance Imaging (MRI) of waterfloods were acquired to determine *in situ* changes in saturation with Berea sandstone and provided an independent measurement of reductions in residual oil saturation by sequential waterflooding. The reductions in residual oil saturation were consistent with those determined previously by volumetric methods.
2. MRI confirmed that sequential flooding, without change in salinity and without cleaning or re-aging of cores with crude oil, gave systematic decrease in residual oil saturation from one waterflood to the next.
3. Changes in the saturation distribution, and in particular the dispersion at the displacement front, indicated that the mechanism of displacement changed from one flood to the next.

ACKNOWLEDGEMENTS

Support for this work was provided by ConocoPhillips, Aramco, BP, Chevron, TOTAL, Shell, StatoilHydro, and the Enhanced Oil Recovery Institute of the University of Wyoming. Special thanks are due to Charles Carlisle and Lonnie Schultz of Chemical Tracers, Inc. We are pleased to acknowledge discussions with Jill Buckley and Xina Xie.

REFERENCES

1. Loahardjo, N., “Improved Oil Recovery by Sequential Waterflooding and by Injection of Low Salinity Brine”, Ph.D. Dissertation, University of Wyoming (2009).
2. Loahardjo, N., Xie, X. and Morrow N.R., ”Oil Recovery by Cyclic Waterflooding of Mixed-Wet Sandstone and Limestone”, presented at the 10th International Symposium on Reservoir Wettability, Abu Dhabi, (2008).
3. Ersland, G.:”Studies of Flow Mechanisms and Hydrate Phase Transitions in Fractured Rocks”, Dissertation, University of Bergen, Norway, (2008).
4. Deans, H. A., “Method of Determining Fluid Saturation in Reservoirs”, U.S. Patent 3623842, (1971).
5. Deans, H. A., Carlisle, C. T., “Single Well Tracer Test in Complex Pore System”, SPE/DOE Symposium on Enhanced Oil Recovery, (1986), SPE 14886.
6. Tang, G.Q., Morrow, N.R., “Salinity, Temperature, Oil Composition and Oil Recovery by Waterflooding”, *SPE Reservoir Engineering*, (1997) **12**, 4, 269-276.
7. Seccombe, J.C., Lager, A., Webb, K.J., Jerauld, G., Fueg, E., “Improved Waterflood Recovery: LoSal™ EOR Field Evaluation”, (2008), SPE 113480.
8. Kumar, M., Senden, T.J., Sheppard, A.P., Middleton, J.P., Knackstedt M.A., “Visualizing and Quantifying the Residual Phase Distribution in Core Material”, presented at the International Symposium of the Society of Core Analyst, Noordwijik, (2009), SCA2009-16.
9. Lebedeva, E., Senden, T.J., Knackstedt, M., Morrow, N.R., “Improved Oil Recovery from Tensleep Sandstone – Studies of Brine-Rock Interactions by Micro-CT and AFM”, presented at the 15th European Symposium of Improved Oil Recovery, Paris, (2009).

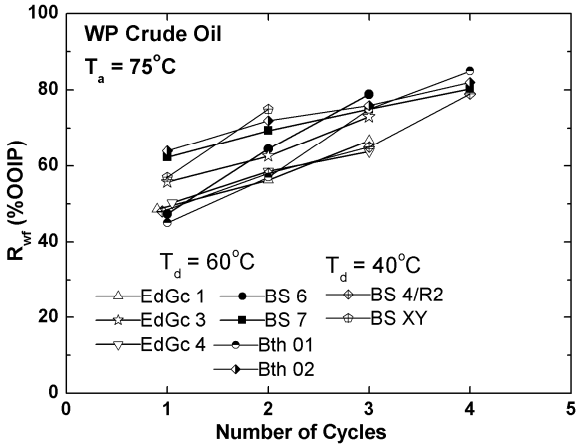

Figure 1. Comparison of recovery of WP crude oil (%OOIP) for Berea (BS) and Bentheim (Bth) sandstone and Edward GC limestone (EdGc) aged at 75°C for 14 days with displacement temperature at 40°C or 60°C. R2 is the second restoration.

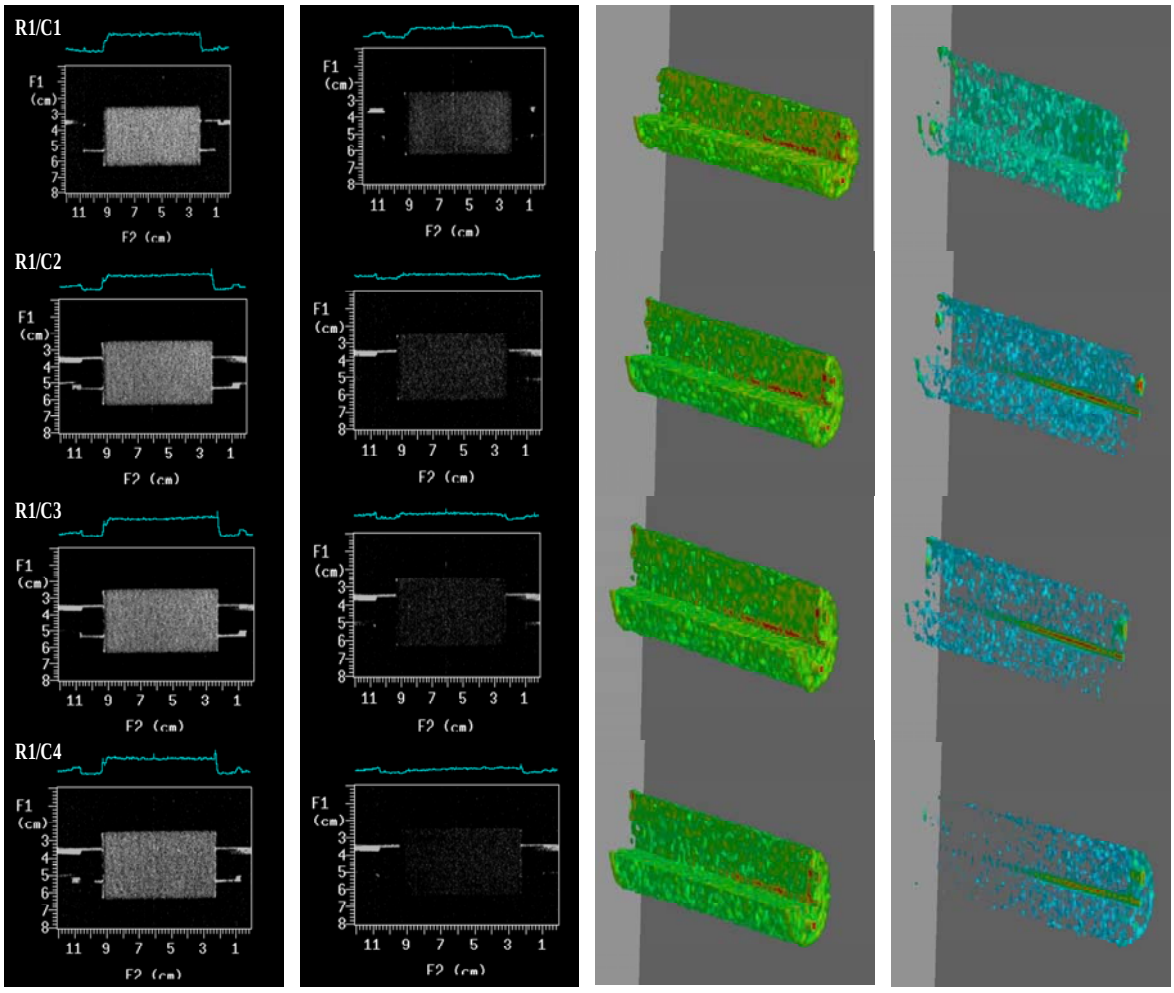

(a) 2D profile at S_{wi} (b) 2D profile at S_{or} (c) 3D profile at S_{wi} (d) 3D profile at S_{or}

Figure 2. 2D and 3D profiles of fluid distribution

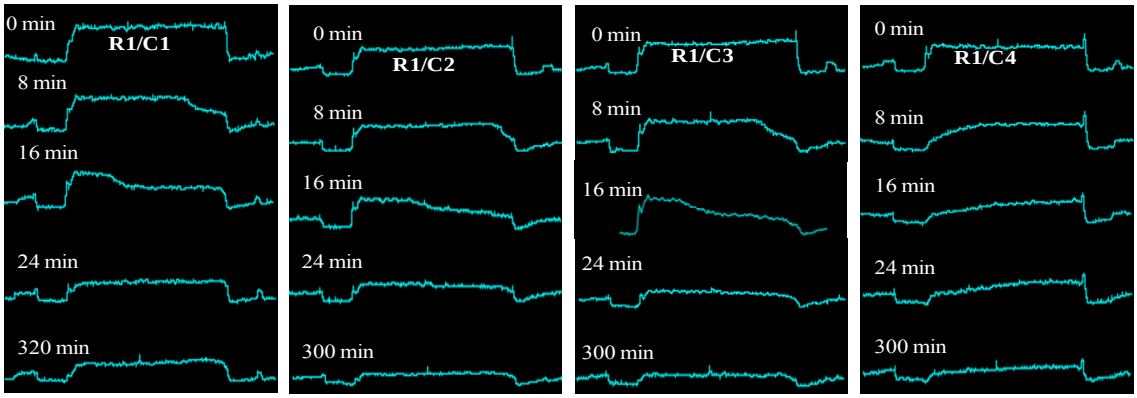

Figure 3. 1D images for waterflooding of R1/C1 through R1/C4; flow direction from right to left except R1/C4 (far right) from left to right

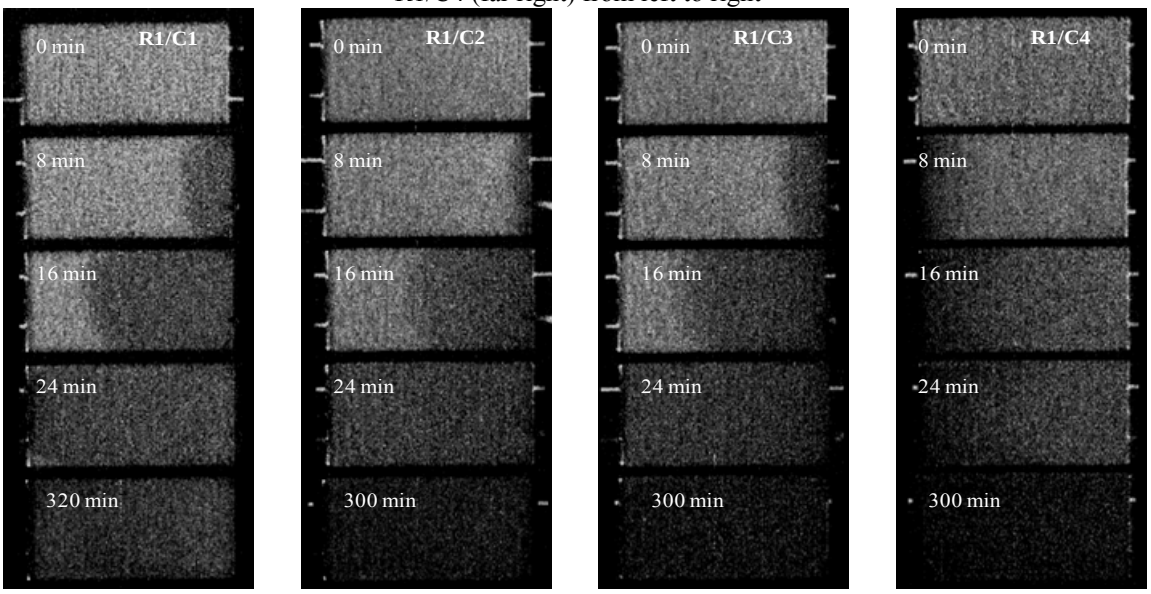

Figure 4. 2D images for waterflooding of R1/C1 through R1/C4; flow direction from right to left except R1/C4 (far right) from left to right

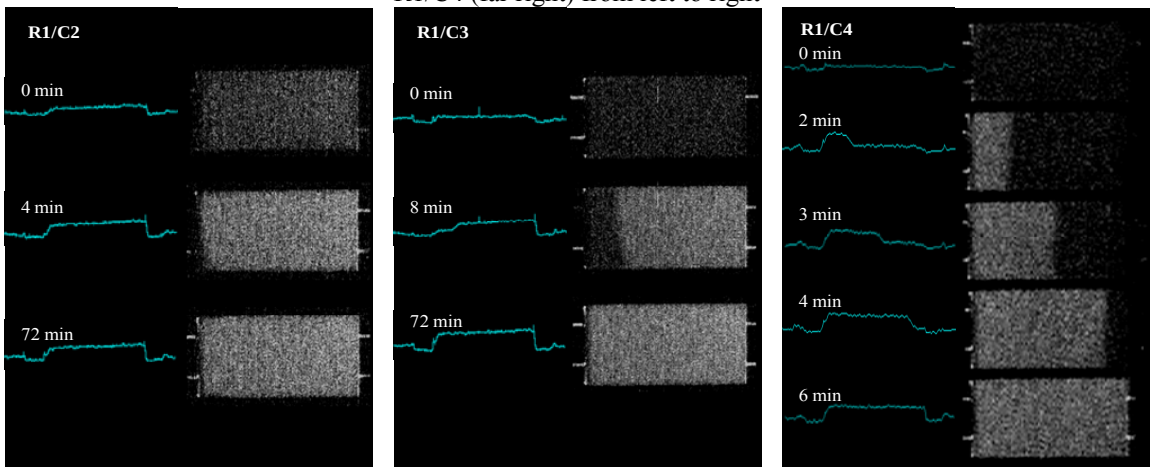

Figure 5. 1D and 2D images for re-establishment of initial water saturation for R1/C2 through R1/C4; flow direction from right to left except R1/C4 (far right) from left to right

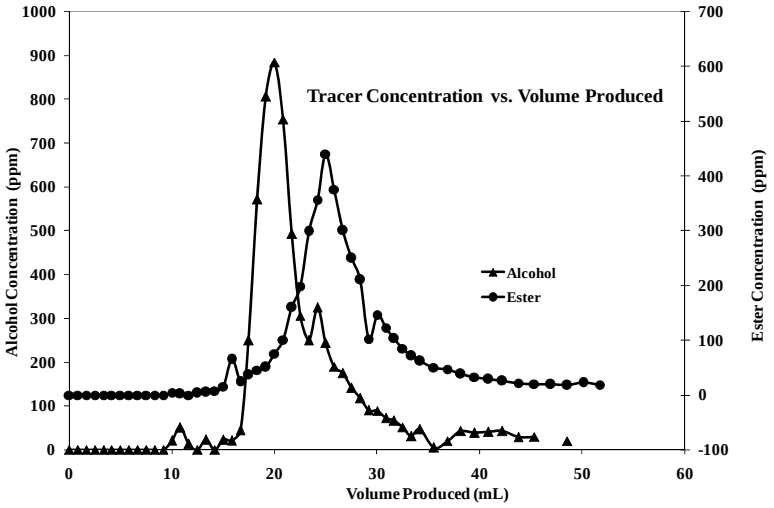

Figure 6. Tracer test data.

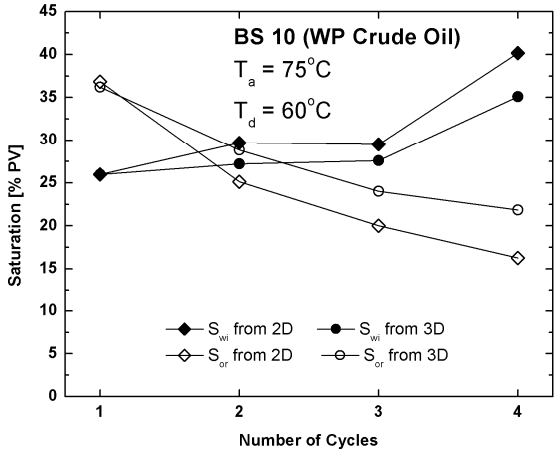

Figure 7. Initial and residual oil saturation for consecutive D_2O-brine for BS 10

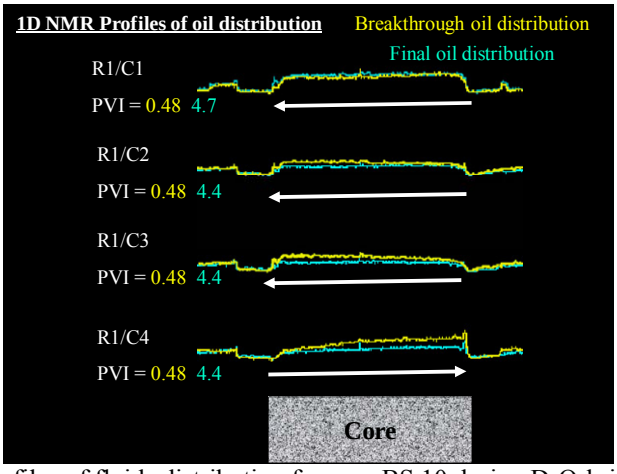

Figure 8. 1D profiles of fluids distribution for core BS 10 during D_2O-brine displacement

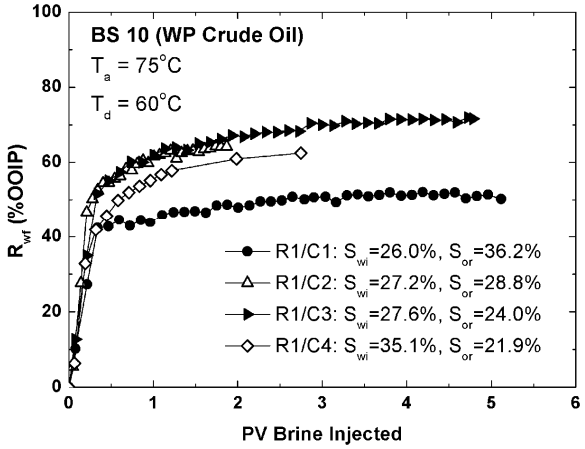

Figure 9. Crude oil recovery for consecutive floods using intensity from MRI

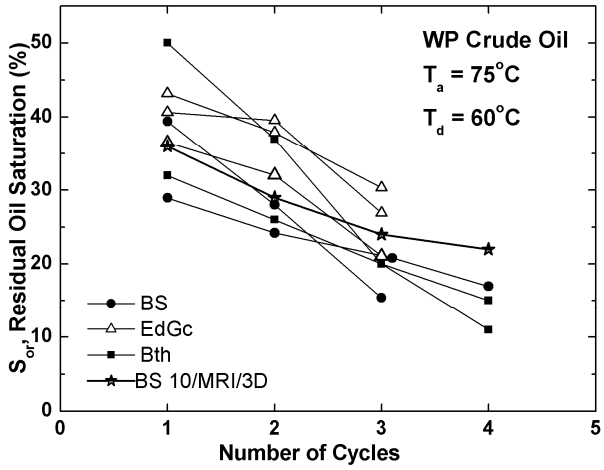

Figure 10. Comparison of residual oil saturation for consecutive D_2O-brine floods at elevated temperature after aging at 75°C for 14 days with coreflood results based on volumetric balance (see Figure 1).

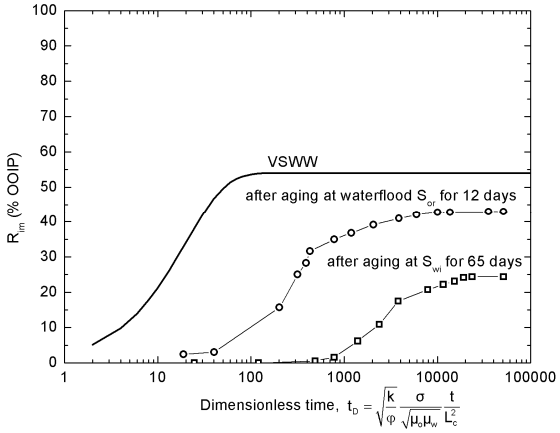

Figure 11. Wettability alteration, by change in aging conditions, indicated by imbibition during sequential waterflooding of Berea sandstone [6].